

# Mineralogical and Geochemical Characterization of Gold-Bearing Minerals from Placers in the Les Saras Area (Mayombe, Congo Republic)

Isidore Nguelet-Moukaha<sup>1,2</sup>, Noël Watha Ndoudy<sup>1,2,3\*</sup>, Jean de Dieu Nzila<sup>1,4</sup>, Claude Dipakama<sup>1,2</sup>, Ulrich Verne Matiaba Bazika<sup>3</sup>, Anne-Sylvie Andre-Mayer<sup>5</sup>, Florent Boudzoumou<sup>3</sup>

<sup>1</sup>Geosciences and Environment Research Laboratory (LARGEN), ENS, Marien Ngouabi University, Brazzaville, Congo

<sup>2</sup>National Forest Research Institute (IRF), Brazzaville, Congo

<sup>3</sup>Faculty of Science and Technology (FST), Marien Ngouabi University, Brazzaville, Congo

<sup>4</sup>Higher Teachers' College (ENS), Marien Ngouabi University, Brazzaville, Congo

<sup>5</sup>GeoResources Laboratory, University of Lorraine-CNRS, Nancy, France

Email: \*nwathandoudy@gmail.com

**How to cite this paper:** Nguelet-Moukaha, I., Watha Ndoudy, N., Nzila, J.D., Dipakama, C., Matiaba Bazika, U.V., Andre-Mayer, A.-S. and Boudzoumou, F. (2025) Mineralogical and Geochemical Characterization of Gold-Bearing Minerals from Placers in the Les Saras Area (Mayombe, Congo Republic). *Open Journal of Geology*, 15, 285-308. <https://doi.org/10.4236/ojg.2025.155014>

**Received:** March 15, 2025

**Accepted:** May 27, 2025

**Published:** May 30, 2025

Copyright © 2025 by author(s) and Scientific Research Publishing Inc. This work is licensed under the Creative Commons Attribution International License (CC BY 4.0).

<http://creativecommons.org/licenses/by/4.0/>



Open Access

## Abstract

With the aim to contribute to the search for the source of placer gold, the Les Saras sector, located in the south-western part of the Republic of the Congo in the Mayombe chain, has been the subject of a study aimed to characterize the mineralogical composition of artisanally mined gold placers. Sediment samples collected from the local drainage system were analyzed using scanning electron microscopy (SEM) and electron microprobe techniques. Results show that the placers are mainly composed of oxides (ilmenite, cassiterite, columbo-tantalite and rutile), followed by silicates (garnets), rare earths (monazite) and native elements (gold). The ilmenites exhibit high TiO<sub>2</sub> (54 - 57 wt%) and FeO (37 - 43 wt%) content, while rutiles are chemically pure. Garnets are classified as almandine- and pyrope-type, and monazites show enrichment in lanthanum (21 - 28 wt%) and cerium (8 - 11 wt%). The angular morphology of gold grains suggests limited transport. Geochemical analyses reveal the presence of Ag, Bi, and Cu as associated elements, along with a peripheral enrichment in gold attributed to selective silver leaching. Two distinct types of gold grains were identified based on fineness: 1) high-fineness grains (up to 988) with low Ag content (<5%), and 2) low-fineness grains (as low as ~670) enriched in Ag (20% - 33%). These compositional differences, along with the geochemical signatures of the associated minerals, suggest two potential sources for the gold: high-temperature hydrothermal systems for the first type and epithermal de-

posits for the second. However, the limited number of analyzed grains for some species points to the need for further analyses, including fluid inclusion studies, to refine the interpretation of the deposit's origin.

## Keywords

Mayombe, Placers, Mineralogy, Geochemistry, Gold

---

## 1. Introduction

Placer deposits, formed through the weathering, transport, and accumulation of materials derived from primary mineral sources, represent a significant source of heavy minerals and precious metals such as gold, platinum, and tin [1]-[6]. These gravity concentrated deposits, commonly found in drainage basins, play a crucial role in mineral exploration due to their relatively easy accessibility and extraction [7] [8]. In Central Africa, placers are often associated with the Precambrian basement, where complex geodynamic processes have influenced mineral distribution. The “Les Saras” area, located in the Mayombe mountain chain in southwestern Republic of the Congo, lies within the eastern segment of the Araçuaí-West Congo Orogen (A-WCO), a geological feature formed by the collision between the Congo and São Francisco cratons [9]-[11]. This region has experienced intense erosion, promoting the development of placer deposits that have been exploited by artisanal miners since the 1930s [12]-[16]. Although previous research has addressed the region's petrography, geochemistry, and geodynamic framework [17]-[22], there remains a lack of detailed studies on the mineralogical assemblages of gold-bearing placers, particularly within the Congolese portion of the Mayombe belt. This gap limits our understanding of their composition, genesis, and depositional history factors that are key to guiding future mineral exploration efforts in the sector. The present study aims to characterize the placer deposits in the Loukenene watershed by identifying the accessory minerals associated with gold and determining their possible sources. The findings will contribute to reconstructing the geological history of these placers and evaluating their economic potential.

## 2. Geological Context

The Mayombe Mountain Range extends from eastern Brazil to the western margins of Central Africa. Studies conducted by [23] and [24] in Brazil, along with research in Angola by [25] and in the Republic of Congo by [18], have demonstrated that the Araçuaí-West Congo Orogen (A-WCO) resulted from the collision between the São Francisco and Congo cratons. This tectonic event led to the formation of Western Gondwana at the end of the Neoproterozoic. Subsequent works by [26]-[30] have delineated the orogen along the African coastline, stretching from western Congo to southwestern Gabon and northwestern Angola (**Figure 1**). In the Republic of the Congo, the lithological assemblage of the Mayombe

range consists of Paleoproterozoic formations in the west, gradually transitioning eastward into Neoproterozoic units [18] [29]-[32].

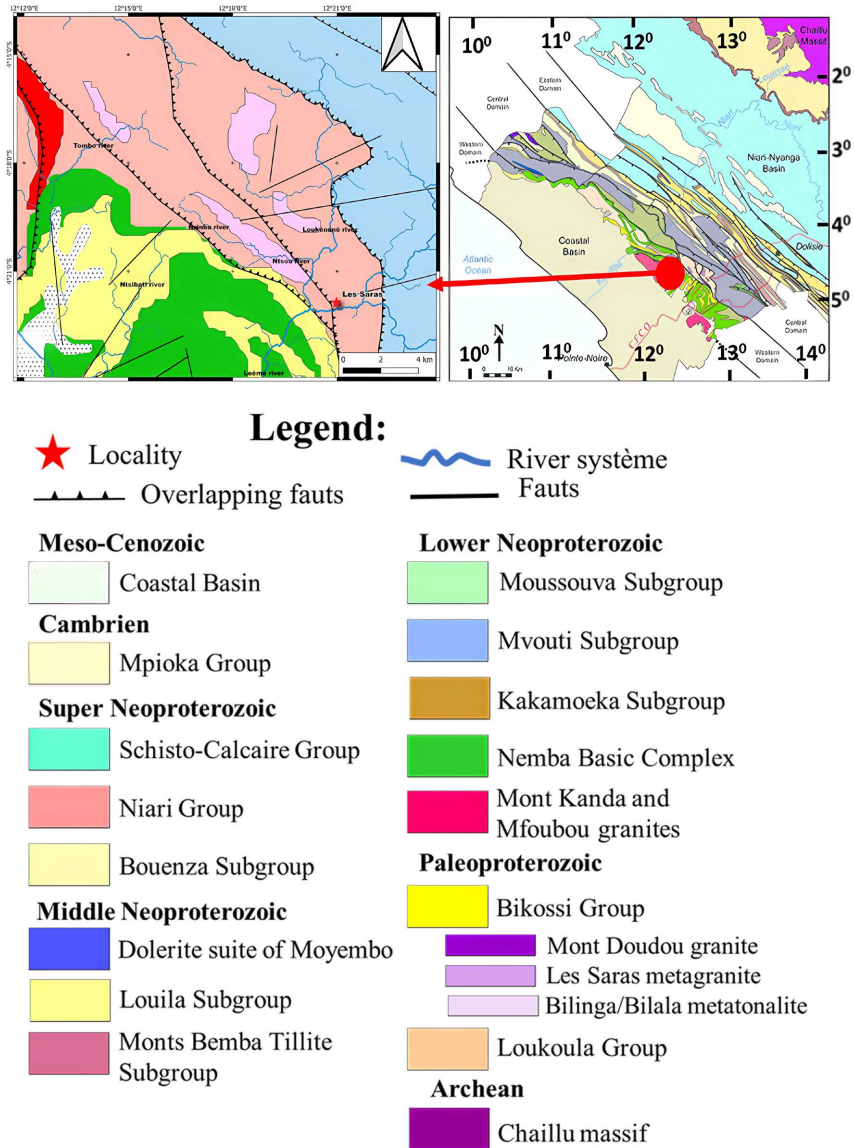


**Figure 1.** Geological map of the study area (adapted from [30], modified by [18] and [33]).

The Mayombe Belt is subdivided into three major domains: the central, western, and eastern domains [18] [26] [27] [33] [34]. The Les Saras sector is located within the western domain, which is composed of Paleoproterozoic formations belonging to the Loémé, Loukoula, and Bikossi groups. According to [31] [32] [35], the Mayombe Group represents a post-rift sequence, consisting of quartzites and schists of the Moussouva subgroup, which include glaciogenic deposits and mudflows composed of black schist matrix embedding clasts and boulders of heterogeneous, sometimes heterometric and heteromorphic rocks. Recent mapping work by [18] indicates that the internal domain of the Mayombe Belt can be sub-

divided into two sectors. The first sector comprises two main groups: The Loémé Group, consisting of schists, ortho- and paragneisses, intersected by the Bilinga and Bilala metagranitoids, and The Loukoula Group, which includes paragneisses, orthogneisses, mica schists, schists, amphibolites, and quartzites, locally intruded by the Les Saras granodiorite [17]. In contrast, the second sector is composed by the Bikossi Group, which covers the study area. This group is characterized by quartzites, quartz schists, metaconglomerates, and, in some areas, mica schists and garnet-bearing schists [18] [26] [31]-[34] [36] and [37]. Studies within this group have identified two distinct mineral assemblages: One composed of garnet-chlorite schists, and Another composed of garnet-biotite schists [33].

### 3. Methodology

In the field, the study involved the collection of samples using the alluvial prospecting method [38] [39]. Sampling was carried out within the hydrographic network of the Les Saras sector, which includes the Loukénééné, Ntsou, Ntsibati, and Tombo rivers (Figure 2).

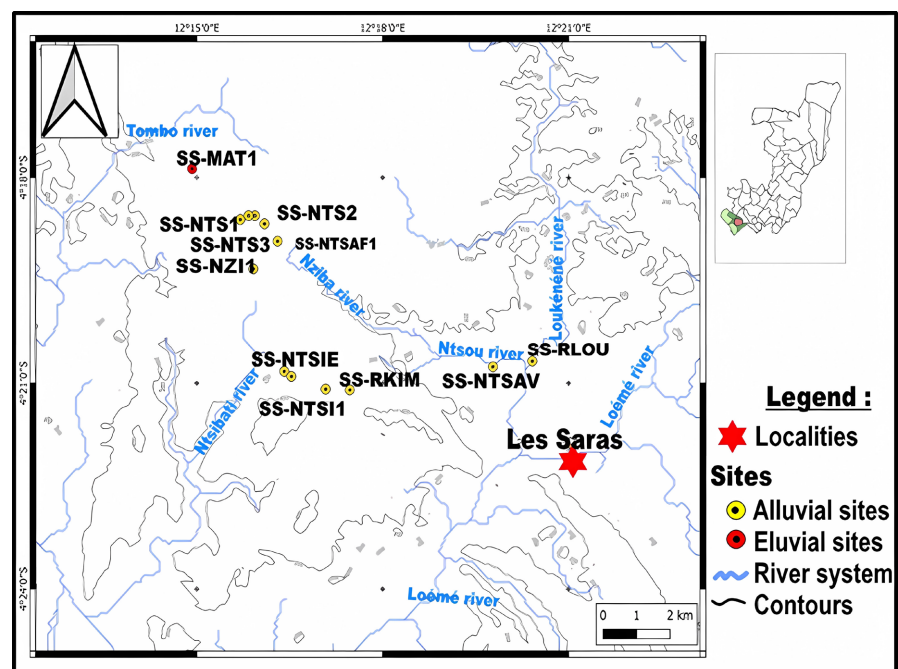


**Figure 2.** Location of sampling points.

The collected samples consisted of panned heavy mineral concentrates obtained from fluvial sediments rich in heavy minerals. These samples were subsequently dried and processed to isolate the heavy fraction using bromoform density separation [38] [40] at the National Institute for Research in Exact and Natural Sciences (IRSEN) in Pointe-Noire.

The heavy mineral description was performed under a binocular microscope (MOTIC RED 30S, 20X - 40X) at the laboratory of the National Institute for For-

estry Research (IRF) in Brazzaville. This stage involved a morphological description and identification of the heavy minerals [39] [41]. Identified minerals were mounted on adhesive slides for further investigation using scanning electron microscopy (SEM) and electron microprobe analysis at the GeoRessources laboratory in Nancy, France.

Semi-quantitative analyses were carried out by X-ray microfluorescence using Bruker's  $\mu$ XRF M4 Tornado, which is able to produce elemental chemical maps. The samples, analyzed without prior preparation, were subjected to a vacuum of 20 mbar. Qualitative analyses were carried out using a JEOL JSM-7600F field emission SEM equipped with an EDS-SDD detector. Analytical conditions included an accelerating voltage of 15 kV and a beam current of 1 nA.

Polished sections were analyzed using a CAMECA SX100 electron microprobe equipped with a wavelength-dispersive spectrometer (WDS) to determine the chemical composition of mineral phases.

The analytical results were normalized and interpreted using geochemical diagrams appropriate to each mineralogical group (oxides, silicates, rare earth minerals, and native elements).

Analyses of the cores of polished gold grains allowed the calculation of gold fineness using the following formula: Fineness (F) =  $(\text{Au}/(\text{Au} + \text{Ag})) \times 1000$  [42] [43], where Au and Ag are the gold and silver contents, respectively. The analytical conditions for microprobe certification of results are listed in **Table 1**.

**Table 1.** Analytical conditions using electron microprobe for samples from the Les Saras sector.

Elt	Line	Spec	Xtal	Peak	Pk Time Bg		Intensity	
					Time Calibration			
					Time/	Repeat		Range/Channels
S	Ka	Sp1	PET	61,448	10	5	Pyrite_20kV_SKa-Sp1-PET_FeKa-Sp3-LIF_001	273.6
Fe	Ka	Sp3	LIF	48,083	10	5	Pyrite_20kV_SKa-Sp1-PET_FeKa-Sp3-LIF_001	205.1
Co	Ka	Sp3	LIF	44,432	20	10	Co_20kV_CoKa-Sp3-LIF_001	505.8
Cu	Ka	Sp5	LLIF	38,325	10	5	Chalcopyrite_20kV_CuKa-Sp5-LLIF_001	505.8
Au	La	Sp5	LLIF	31,764	20	10	Au_20kV_AuLa-Sp5-LLIF_001	277.9
Ni	Ka	Sp5	LLIF	41,219	20	10	Ni_20kV_NiKa-Sp5-LLIF_001	1096.0
Zn	Ka	Sp3	LIF	35,640	20	10	ZnS_20kV_ZnKa-Sp3-LIF_001	250.2
As	La	Sp2	TAP	37,604	20	10	AsGa_20kV_AsLa-Sp2-TAP_001	209.2
Ag	La	Sp4	PET	47,489	20	10	Ag_20kV_AgLa-Sp4-PET_001	144.9
Sb	La	Sp1	PET	39,307	20	Sp1	Sb2S3_20kV_SbLa-Sp1-PET_001	291.7
Pb	Ma	Sp4	PET	60,435	20	10	Galène_20kV_PbMa-Sp4-PET_001	77.7
Bi	Ma	Sp1	PET	58,517	20	10	Bi_20kV_BiMa-Sp1-PET_001	129.3

Elt: element; Spec: spectrum.

## 4. Results

### 4.1. Description and Identification of Heavy Minerals

From the 4170 heavy mineral grains analyzed for the Les Sarras gold placers, cassiterite is the most abundant at all sites, followed by garnet, ilmenite, rutile, columbite-tantalite, monazite and gold (Figure 3).

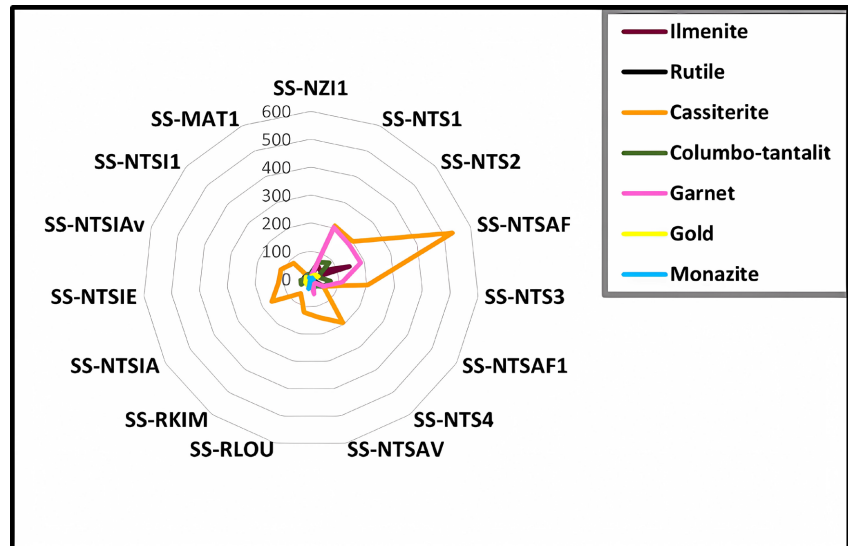


Figure 3. Grain count by mineral species according to the sites.

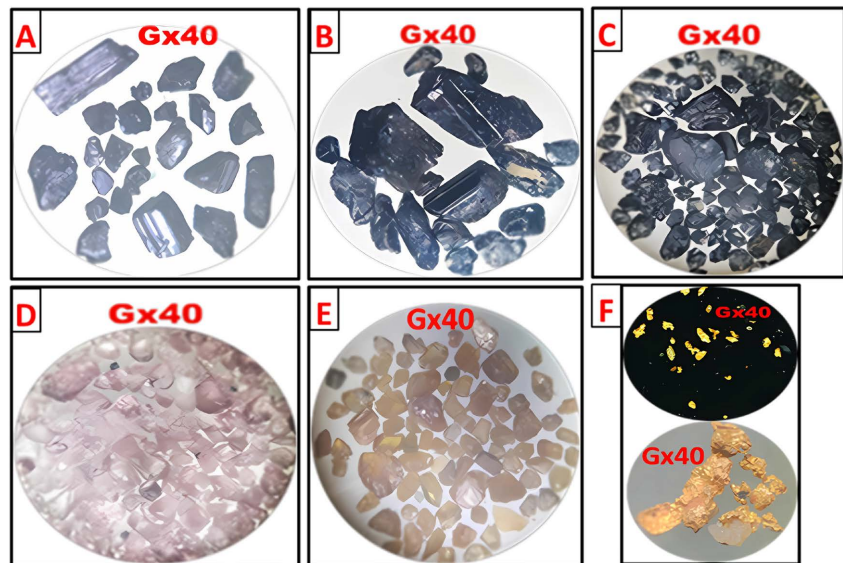


Figure 4. Morphological characteristics of the studied grains: (A) Ilmenite, (B) Rutile, (C) Cassiterite, (D) Garnet, (E) Monazite, and (F) Gold.

The description and identification of mineral species were based on their morphological characteristics (transparency, color, shape/section, luster, and other features). Based on these criteria, seven mineral species were identified: four species from the oxide group (ilmenite, rutile, cassiterite, and columbo-tantalite), one

species from the silicate group (garnet), one species from the rare earth elements group (monazite), and one species from the native elements group (gold). Ilmenites are opaque, dark grey in color, elongated rhombohedral tablets with longitudinal striations; the edges are either sharp or sub-angular; the luster is metallic, and the grains are very weakly magnetic (**Figure 4(A)**). Rutile grains are opaque, dark-gray prisms with an elongated, flattened shape and a metallic luster (**Figure 4(B)**). Cassiterite grains are opaque, dark brown, angular in shape, with a metallic luster, displaying both longitudinal and transverse striations (**Figure 4(C)**). Garnets are translucent, pink in color, sub-angular and elongated in shape, with a vitreous luster (**Figure 4(D)**). Monazites are translucent, yellow brown in color, sub-angular and elongated, with a greasy to vitreous luster (**Figure 4(E)**). Gold grains are opaque, metallic yellow in color, flattened, sub-crystalline, with very irregular outlines, a metallic luster, and show phenomena of peptization, quartz grain inclusions, and impact marks (**Figure 4(F)**).

## 4.2. Geochemistry of Heavy Minerals

Geochemical analyses show that the placers are dominated by oxides, notably ilmenite, cassiterite, columbo-tantalite, and rutile.

### 4.2.1. Oxides Group

The oxides are dominated, in order of abundance, by cassiterite, ilmenite, rutile, and columbotantalite. The cassiterite grains, with an average composition of 97.3% by weight of  $\text{SnO}_2$ , exhibit trace amounts of significant concentrations of Nb and Ta. The niobium pentoxide ( $\text{Nb}_2\text{O}_5$ ) shows average concentrations of 0.2% by weight, tantalum pentoxide ( $\text{Ta}_2\text{O}_5$ ) 0.33% by weight, MnO 0.03% by weight, and FeO 0.18% by weight (**Table 2**). Normalization to Apfu reveals a bimodal distribution of trace elements, suggesting a dual origin (magmatic and metamorphic). Ilmenites show average concentrations of 56.4% by weight of  $\text{TiO}_2$ , and 41.4% by weight of FeO. The trace elements indicate an abundance of tungsten oxide ( $\text{WO}_3$ ) at 0.11% by weight, uranium oxide ( $\text{UO}_2$ ) at 0.04%, and chromium oxide ( $\text{Cr}_2\text{O}_3$ ) at 0.02% by weight (**Table 2**). Furthermore, the presence of zirconium oxide ( $\text{ZrO}_2$ ) at an average concentration of 0.06% by weight suggests the presence of zinciferous ilmenites in the area [44]. Zinciferous ilmenite develops during contact metamorphism associated with granite intrusions [44]. The  $\text{TiO}_2$  content of rutile reaches an average of 96.5% by weight. The trace elements identified in rutile grains show average concentrations of 0.97% by weight of iron, 0.69% by weight of niobium, and 0.04% by weight of tantalum (**Table 2**). The presence of these elements helps determine the origin and formation conditions of the rutile.

Ilmenites exhibit very low proportions of MnO and MgO (ranging from 0.4 to 3 wt% and 0.02 to 0.2 wt%, respectively), suggesting a possible partial substitution of  $\text{Fe}^{2+}$  by  $\text{Mg}^{2+}$  and  $\text{Mn}^{2+}$  within the ilmenite structure (**Figure 5(A)**). However, this substitution is more strongly influenced by increasing temperature than by pressure during metamorphism [44].

**Table 2.** Average chemical composition of oxides in % by weight analysed in the Les Saras sector.

Analyses (W%)	Ilmenite (N = 25)	Rutile (N = 23)	Cassiterite (N = 25)
TiO <sub>2</sub>	55.7	96.5	0.03
FeO	40.89	1.01	0.19
MnO	1.27	0.04	0.03
MgO	0.12	0.05	0.12
Nb <sub>2</sub> O <sub>5</sub>	0.09	0.72	0.21
Ta <sub>2</sub> O <sub>5</sub>		0.04	0.35
SnO <sub>2</sub>		0.03	98
ZrO <sub>2</sub>	0.06	0.13	
Al <sub>2</sub> O <sub>3</sub>	0.32	0.1	1.12
SiO <sub>2</sub>	0.11	0.04	0.25
Cr <sub>2</sub> O <sub>3</sub>	0.02	0.17	0.02
WO <sub>3</sub>	0.11	1.18	
UO <sub>2</sub>	0.04	0.13	0.04
CaO			0.37
Ce <sub>2</sub> O <sub>3</sub>			0.07
Total	98.73	100.14	100.80

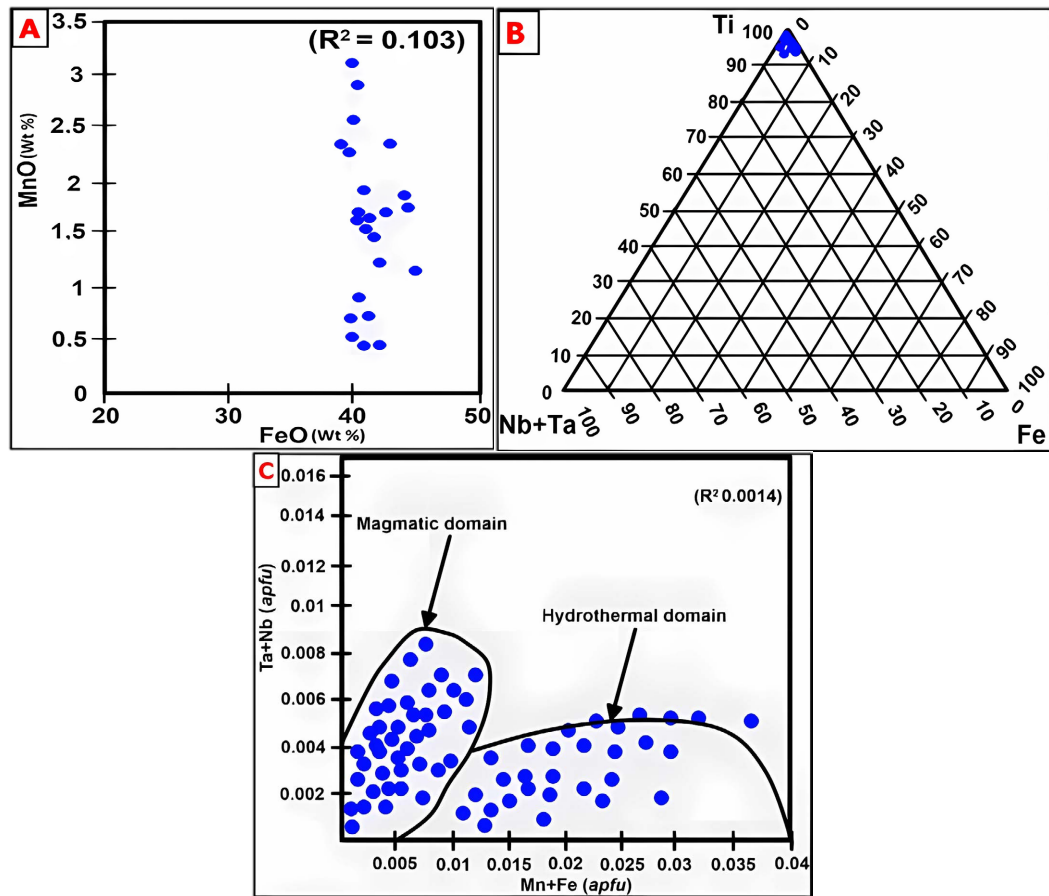


**Figure 5.** (A) Binary diagram showing the contents (wt%) of MnO vs FeO% in ilmenite grains; (B) Ternary diagram showing the contents (wt%) of Ti, Fe and Nb + Ta in rutile grains; (C) Binary diagram showing the distribution of Mn + Fe vs Ta + Nb content of normalized trace elements (APFU) in cassiterite grains.

FeO is present in low concentrations (0.2 to 3 wt%) in rutile, along with trace amounts of Nb<sub>2</sub>O<sub>5</sub> and ZrO<sub>2</sub>, suggesting high-pressure formation conditions (**Figure 5(B)**).

High concentrations of Mn and Fe are observed in some cassiterite grains, while others show elevated Nb and Ta contents (**Figure 5(C)**). This may reflect distinct hydrothermal and magmatic origins.

The analyzed columbo-tantalite grains reveal two distinct groups. The first group is characterized by very high concentrations of niobium pentoxide (Nb<sub>2</sub>O<sub>5</sub>), ranging from 67.8 to 71.18 wt%, and low concentrations of tantalum pentoxide (Ta<sub>2</sub>O<sub>5</sub>), between 4.5 and 6.4 wt% (**Figure 6**). The second group shows high Ta<sub>2</sub>O<sub>5</sub> contents, ranging from 62.21 to 75.28 wt%, and lower Nb<sub>2</sub>O<sub>5</sub> contents, between 7.42 and 10.10 wt% (**Table 3**).

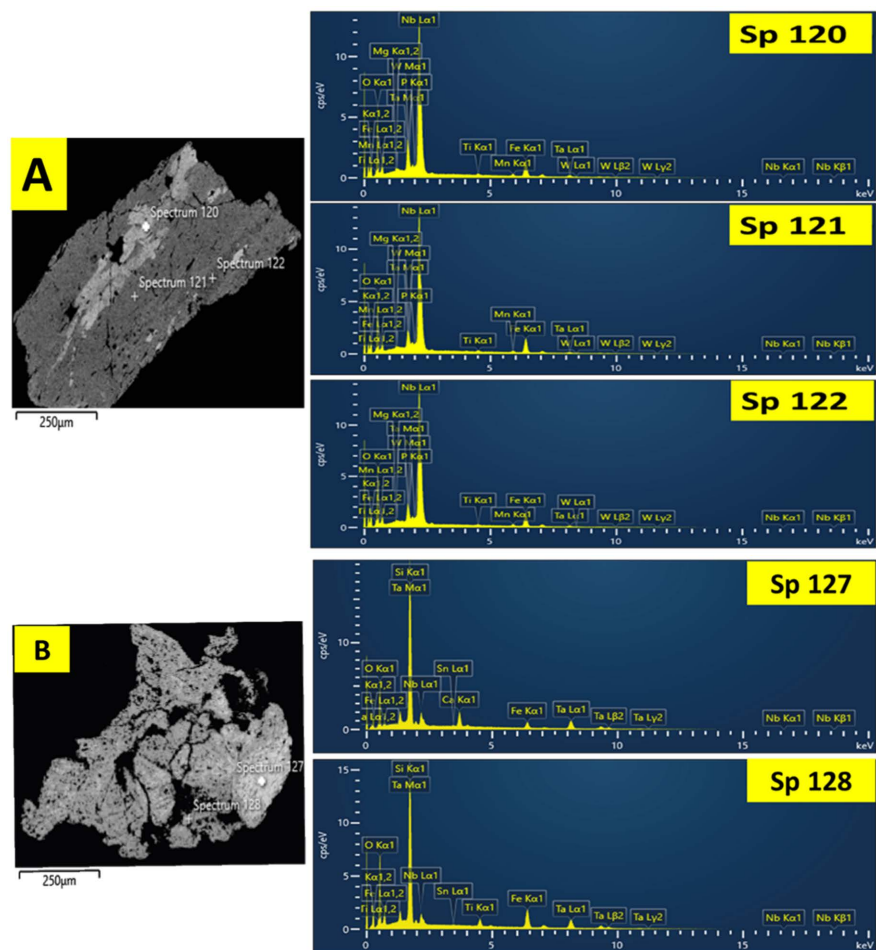


**Figure 6.** Chemical composition of columbite-tantalite grains observed by SEM. (A) Niobium-rich Columbo-tantalite grain, Sp 120, Sp 121 and Sp 122 analysis spectra; (B) Tantalum-rich columbite-tantalite grain, Sp 127 and Sp 128.

The niobium and tantalum contents suggest the presence of two distinct columbo-tantalite populations. One is niobium-rich (columbite), with FeO contents ranging from 16.33 to 16.63 wt%, corresponding to the ferrocolumbite group. The

other is tantalum-rich (tantalite), with FeO contents between 14.03 and 18.46 wt%, representing the ferrotantalite group [45]. The TiO<sub>2</sub> concentrations (0.75 - 0.85 wt%) in the first three samples and those (0.22 - 9.99 wt%) in the last two, along with Mn# values (7.80 - 8.62) for the first group and Ta# values (84.43 - 89.93) for the second, suggest a diversity of origins for the columbo-tantalite [46] [47]. This diversity may be linked to granite intrusions (Les Saras granite and Mfoubou granite) previously reported in the area by [17]-[22]. The second group could serve as a guide for tantalum exploration in the sector.

**Table 3.** Chemical composition of Colombo-tantalite grains normalised to 6 oxygen atoms.

Analyses	SS-NTS1	SS-NTS2	SS-NTS3	SS-NTSAF1	SS-NTSIA
	Colombite	Colombite	Colombite	Tantale	Tantale
TiO <sub>2</sub> -W%	0.75	0.88	0.85	0.22	9.99
SnO <sub>2</sub>	-	-	-	0.96	0.54
FeO	16.63	16.53	16.33	14.03	18.46
MnO	1.39	1.54	1.44	0.24	0.01
Ta <sub>2</sub> O <sub>5</sub>	7.29	10.1	7.42	75.28	62.21
Nb <sub>2</sub> O <sub>5</sub>	71.14	67.8	71.18	8.35	4.19
ZrO <sub>2</sub>	0.16	0.12			
Al <sub>2</sub> O <sub>3</sub>	-	0.08	0.32	0.59	0.43
WO <sub>3</sub>	1.24	1.29	1.81	0.21	0.28
MgO	0.39	0.43	0.47	0.08	0.1
Total	98.99	98.77	99.82	99.96	96.21
Al-apfu	0.0	0.0	0.0	0.0	0.0
Site A	0	0	0	0	0
Fe	0.81	0.82	0.79	0.94	1.17
Mn	0.07	0.08	0.07	0.02	0.00
Mg	0.00	0.00	0.00	0.00	0.00
Site B	0.88	0.9	0.86	0.96	1.17
Ti	0.03	0.04	0.04	0.01	0.57
Sn	0.00	0.00	0.00	0.03	0.02
Ta	0.12	0.16	0.12	1.64	1.29
Nb	1.88	1.82	1.86	0.30	0.14
Zr	0.00	0.00	0.00	0.00	0.00
W	0.00	0.00	0.00	0.00	0.00
Site C	2.03	2.02	2.02	1.98	2.02
Total	2.91	2.92	2.88	2.94	3.19
Ta# Ta/(Ta + Fe)	5.81	8.22	5.90	84.43	89.93
Mn# Mn/(Mn + Nb)	7.80	8.62	8.20	1.70	0.05

Apfu: Analyses of Atoms per Formula Unit.

#### 4.2.2. Silicate Group

Among the silicate group, only garnet was analyzed. The results show that the

garnets exhibit high FeO contents (29 - 36 wt%) and MgO contents (3 - 6 wt%) (**Table 4**), along with low MnO (1.0 - 1.3 wt%) and CaO (1.0 - 1.09 wt%) contents, indicating that the garnets are depleted in  $Mn^{2+}$  and  $Ca^{2+}$ .

**Table 4.** Chemical composition of garnet grains analysed on the basis of 12 carbon atoms.

Analyses	SS-NTS2	SS-NTS1	SS-NTSAF	SS-NTS3	SS-NTSAF1	SS-NTSAV	SS-NTSIE	SS-NTS4	SS-NTSIAV
	Grenat	Grenat	Grenat	Grenat	Grenat	Grenat	Grenat	Grenat	Grenat
SiO <sub>2</sub> -W%	38.96	56.07	37.97	38.96	56.07	37.19	38.17	37.96	39.14
Al <sub>2</sub> O <sub>3</sub>	19.21	10.45	21.94	19.21	10.43	20.97	20.17	19.49	19.81
FeO	33.65	28.85	31.83	33.63	28.85	35.56	35.12	35.66	34.47
MnO	0.762	0.45	1.3	0.76	0.44	0.57	0.82	0.87	0.92
MgO	6.42	3.41	5.86	6.42	3.41	4.77	4.89	4.97	4.62
CaO	1.02	1.01	1.09	1.02	1.02	0.95	0.89	1.09	1.01
Na <sub>2</sub> O	0	0.02	0	0	0.02	0	-0.01	0.019	0.02
K <sub>2</sub> O	-0.01	-0.03	0	-0.01	0.02	-0.03	-0.01	0	-0.01
P <sub>2</sub> O <sub>5</sub>	0	0	0	0	0	0	0	0	0
TiO <sub>2</sub>	0.01	0.16	0	0.01	0.17	0.01	-0.04	-0.01	0.02
Total	100	100	100	100	100	100	100	100	100
Ca-apfu	0.09	0.08	0.09	0.09	0.08	0.08	0.08	0.09	0.09
Si	3.09	4.18	2.99	3.09	4.18	2.98	3.05	3.05	3.11
Al	1.8	0.92	2.04	1.8	0.92	1.98	1.9	1.84	1.86
Fe	2.23	1.8	2.1	2.23	1.8	2.38	2.35	2.39	2.29
Mn	0.05	0.03	0.09	0.05	0.03	0.04	0.06	0.06	0.06
Mg	0.76	0.38	0.69	0.76	0.38	0.57	0.58	0.59	0.55
%Almandin	71.3	78.7	70.7	71.3	78.7	77.5	76.7	76.4	76.7
%Pyrope	24.3	16.6	23.2	24.3	16.6	18.5	19.0	18.7	18.3
%Grossulaire	2.8	3.5	3.1	2.8	3.5	2.7	2.5	3.0	2.9
%Spessartine	1.6	1.1	2.9	1.6	1.1	1.3	1.8	1.9	2.1

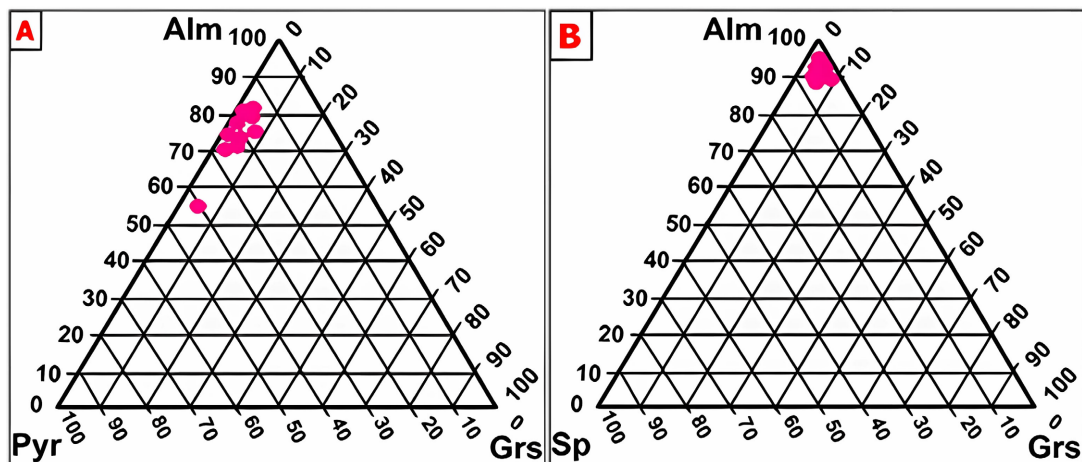


**Figure 7.** Position of the garnets analysed in the ternary diagrams of [49] [50]: (A) almandine-pyrope-grossulaire and (B) almandine-spessartine-grossulaire (normalised apfu content).

These compositions suggest that the garnets are primarily of the almandine (Alm) and pyrope (Pyr) types (**Figure 7**). Trace elements include low concentrations of MnO and CaO (1.0 - 1.27 wt% and 1.0 - 1.07 wt%, respectively), confirming their metamorphic origin [48].

#### 4.2.3. Rare Earths Group

The rare earth element group is represented by monazite. Monazite grains are enriched in  $P_2O_5$  (29 - 37 wt%) and exhibit high concentrations of lanthanum (21 - 28 wt%) and cerium (8 - 11 wt%). The weak correlation between CaO and  $P_2O_5$  concentrations suggests chemical zoning, reflecting variations in the formation environment (**Figure 8**).

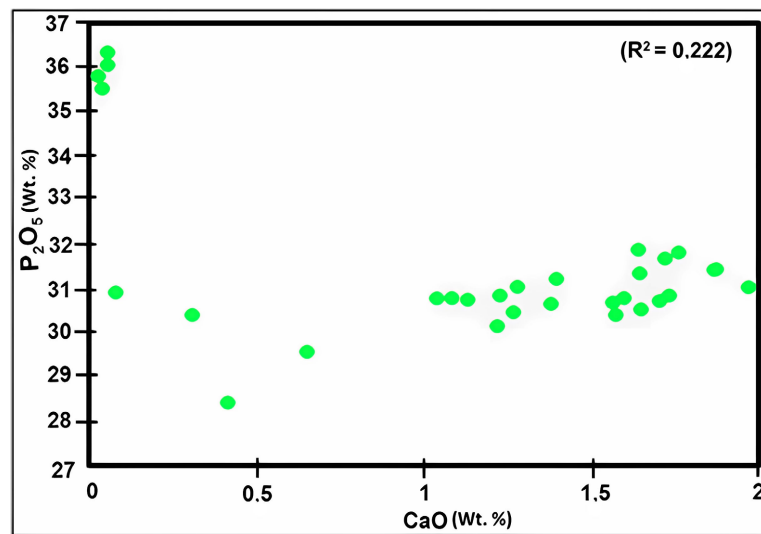


**Figure 8.** Binary diagram  $P_2O_5$  vs CaO showing the distribution of concentrations in monazite grains in wt%.

#### 4.2.4. Native Elements Group

Gold is the principal native element observed in the Les Saras placers. The gold grains exhibit well-defined angular features (**Figure 9**).

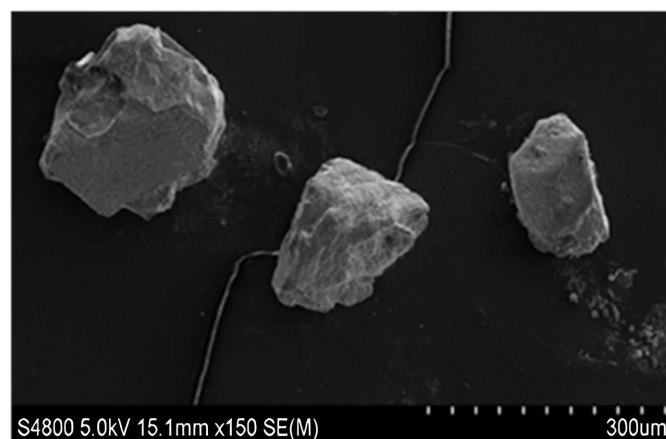


**Figure 9.** SEM angular gold grains.

**Table 5.** Electron microprobe chemical analysis results of gold grains.

Samples	Mineral	Results (wt%)								Fineness (Au/(Au + Ag))*1000	Au/Ag
		Au	Ag	Bi	As	Cu	Fe	Co	Sb		
1-L1-1C	Electrum	75.66	23.79	0.54	0.00	0.00	0.00	0.00	0.00	761	3.2
1-L1-2C	Electrum	75.69	23.04	0.67	0.00	0.00	0.00	0.00	0.00	767	3.3
1-L1-3C	Native gold	96.24	2.79	0.76	0.00	0.00	0.00	0.00	0.00	972	34.5
1-L1-4C	Native gold	88.67	11.81	0.73	0.02	0.32	0.00	0.00	0.00	882	7.5
1-L1-5C	Native gold	88.25	11.7	0.7	0.02	0.32	0.00	0.00	0.00	883	7.5
1-L1-6C	Electrum	67.74	33.42	0.42	0.01	0.00	0.00	0.00	0.00	670	2.0
1-L1-7C	Native gold	96.98	1.35	0.99	0.02	0.67	0.00	0.00	0.00	986	71.8
1-L1-8C	Native gold	97.02	1.13	0.55	0.02	0.66	0.00	0.00	0.00	988	85.9
1'-L1-9C	Native gold	98.47	1.85	0.82	0.01	0.00	0.00	0.00	0.00	982	53.2
1'-L1-10C	Native gold	88.56	11.01	0.73	0.00	0.00	0.00	0.00	0.00	889	8.0
1'-L1-11C	Native gold	97.3	2.95	0.71	0.00	0.03	0.02	0.00	0.00	971	33.0
1'-L1-12C	Native gold	97.76	2.3	0.57	0.00	0.02	0.00	0.00	0.00	977	42.5
1'-L1-13C	Native gold	84.48	16.81	0.63	0.00	0.00	0.00	0.00	0.02	834	5.0
1'-L1-14C	Electrum	79.52	21.86	0.74	0.00	0.00	0.00	0.00	0.00	784	3.6
1'-L1-15C	Native gold	81.47	19.02	0.52	0.00	0.00	0.00	0.00	0.06	811	4.3
1'-L1-16C	Native gold	94.94	6.39	0.68	0.00	0.00	0.00	0.00	0.00	937	14.9
1'-L1-17C	Native gold	94.75	5.01	0.69	0.00	0.03	0.00	0.00	0.02	950	18.9
1'-L1-18C	Electrum	78.36	22.28	0.48	0.00	0.00	0.00	0.00	0.00	779	3.5
1'-L1-19C	Native gold	83.52	16.91	0.64	0.00	0.00	0.00	0.00	0.00	832	4.9
1'-L1-20C	Electrum	77.45	24.01	0.64	0.00	0.00	0.00	0.00	0.00	763	3.2
1'-L1-21C	Native gold	92.04	8.08	1.01	0.01	0.00	0.00	0.00	0.00	919	11.4
1'-L1-22C	Native gold	92.01	8.89	0.94	0.00	0.00	0.00	0.00	0.00	912	10.3
1'-L1-23C	Native gold	91.27	8.91	0.68	0.00	0.00	0.00	0.03	0.00	911	10.2
1'-L1-24C	Native gold	92.53	7.87	0.54	0.00	0.00	0.00	0.00	0.00	922	11.8
Min		67.74	1.13	0.42	0.00	0.00	0.00	0.00	0.00	670	59.9
Maxi		98.47	33.42	1.01	0.02	0.67	0.02	0.03	0.06	988	2.9
Moyenne		87.94	12.22	0.68	0.005	0.09	0.001	0.001	0.004	878	7.2

The chemical composition of gold grains from the Les Saras area (**Table 5**) reveals that the gold is primarily alloyed with silver, bismuth, copper, and traces of arsenic, cobalt, and antimony. The gold (Au) content in the analyzed grains ranges from 67.74% to 98.47%, with a high average of 87.94%. Conversely, silver (Ag) content varies inversely from 1.13% to 33.42%, with an average of 12.22%. This negative correlation between gold and silver contents reflects a wide compositional range, from nearly pure gold to silver-rich electrum. A similar inverse relationship is observed between fineness and silver content: the higher the Ag content, the lower the fineness. This relationship is expected, as fineness is directly

defined by the relative proportion of gold in the alloy, making it a key indicator for estimating the formation temperatures of gold grains [51]. **Figure 10** illustrates this relationship between gold and silver contents and inferred formation temperatures. The data points from the Les Saras samples are distributed primarily between the medium- and high-temperature fields, indicating variability in metallogenic conditions. This trend supports previously suggested differences in formation contexts [20]-[22]. Bismuth (Bi) is detected in low amounts, ranging from 0.42% to 1.01%, suggesting a minor association with hydrothermal processes [43] [51] [52]. Additionally, trace elements such as arsenic (As), copper (Cu), iron (Fe), cobalt (Co), and antimony (Sb) are present in concentrations below 0.1%. Although their levels are low—which is typical for native gold—their presence remains significant, as they provide insight into the formation conditions of the auriferous mineralizations (**Figure 10**). In this study, the fineness of the gold grains ranges from 670 to 988, with an average of 878 (**Table 5**). Fineness values below 800 correspond to silver-rich electrum, while values above 900 indicate nearly pure gold. This bimodal or scattered distribution suggests multiple primary sources for the gold grains, implying at least two distinct types of deposits [51] [52]. Regarding the Au/Ag ratio, values range widely from 2.0 to 85.9, with an average of 7.2. This ratio is a useful indicator of the nature and origin of the gold [51]-[53]: high values (>30) are indicative of very pure gold, typically associated with hypogene deposits, whereas low values (~2 - 4) are characteristic of silver-rich electrum, which may originate from polymetallic sulfide deposits or near-surface altered zones [52].

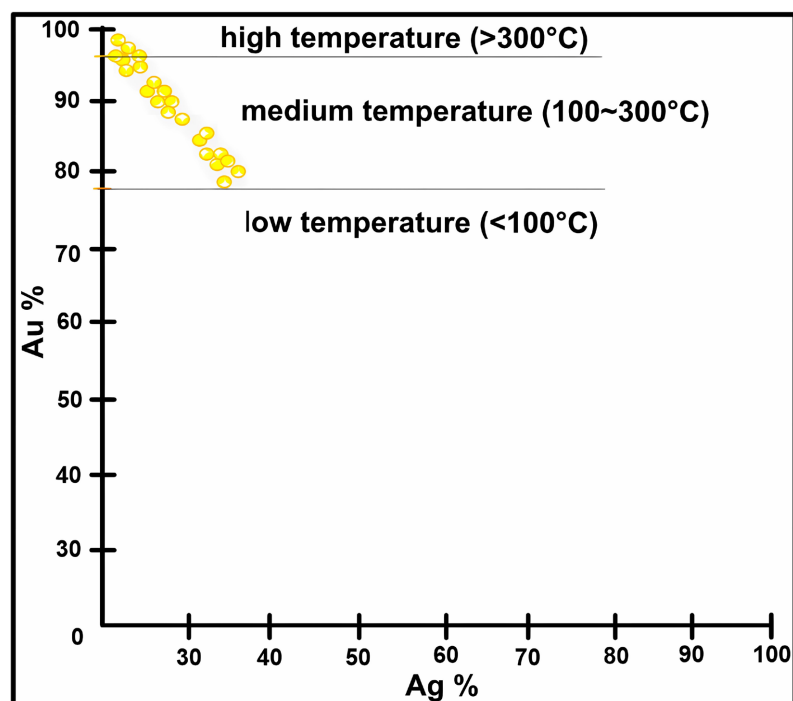


**Figure 10.** Position of Les Saras gold grains in the correlation diagram between gold and silver content and mineralization temperature [51].

**Table 6** shows that at the grain boundaries, the gold content varies from 50.6% to 100% (average 93%), silver content ranges from 0.16% to 49.1% (average 7%), and bismuth content varies from 0.46% to 0.9% (average 0.72%). The composition suggests leaching of the chemical elements accompanying the gold [51]-[53].

**Table 6.** Results of chemical analysis of gold grains (analysed in the centre and at the edge).

Chemical composition	Nb 165	Au	Ag	Bi	As	Cu	Sb
Mean Centre		88	12.2	0.68	0	0.09	0
Standard deviation		8.53	8.88	0.15	0.01	0.2	0.01
Min		67.7	1.13	0.42	0	0	0
Max		98.5	33.4	1.01	0.02	0.67	0.02
Mean Edge		93.4	6.96	0.72	0	0	0.01
Standard deviation		11.2	11.1	0.13	0.01	0.01	0.02
Min		50.6	0.16	0.46	0	0	0
Max		100	49.1	0.9	0.02	0.04	0.05

## 5. Discussion

The interpretation of this study's results will focus on the origin and emplacement mechanisms of the Les Saras gold placers. Subsequently, prospects for mineral exploration will be outlined.

### 5.1. Mineral Characterization and Origin

Geochemical analyses show that the minerals accompanying the gold in the Les Saras placers provide information about the phenomena that led to the genesis of the source rocks.

- **Oxides**

The ilmenites rich in TiO<sub>2</sub> and FeO, along with the nearly pure rutile, indicate high-temperature and high-pressure metamorphism, as previously demonstrated in the work of [18] on the Mayombe. The cassiterites, on the other hand, exhibit a dual origin: grains enriched in Nb and Ta suggest a magmatic origin, while those rich in Mn and Fe point to a hydrothermal contribution [54]. The columbotantalites display reasonable concentrations of niobium and tantalum in the grains, but the small number of grains analyzed does not allow for hypotheses to be made regarding their origins.

- **Silicates and rare earths**

Almandine-pyrope garnets and monazites enriched in lanthanum and cerium confirm high-temperature metamorphism [48]-[50] and [54]. The zonations observed in monazite grains reflect variations in chemical composition linked to distinct crystallization cycles.

- **Gold**

The strongly angular morphology of the gold grains indicates limited transport within the basin, as suggested by the works of [55]-[62]. The geochemical signa-

ture, predominantly composed of Au, Ag, Bi, Cu, and Sb, reveals chemical homogeneity at the core of the grains and an enrichment in gold at the boundaries compared to the center. This phenomenon is attributed to the selective dissolution of the gold's accompanying elements in the grains [63] [64]. The geochemical signature of the gold grains in the Les Saras area, along with their fineness, suggests a dual origin:

- A hydrothermal origin, as confirmed by the characteristics visible in **Figure 11**, typical of epithermal gold-rich deposits. Such deposits are well documented in China [51], Russia [57], Canada [60] [64], Chile [65], as well as in Mayombe, where they are considered by [33]. This hypothesis aligns with the conclusions of [15], made on a larger scale across the Mayombe chain.
- A differentiated thermometric origin, revealed by the analysis of the gold fineness: fineness values below 800 correspond to argentiferous electrum, typically formed in low-temperature epithermal environments [51] [52] [64]. Conversely, values above 900 indicate nearly pure gold, typical of mesothermal to hypothermal genesis, meaning at higher temperatures and depths [64] [66] [67].

These two types of signatures suggest the existence of at least two primary sources, corresponding to two distinct types of deposits. This hypothesis is further supported by the simultaneous observation of two types of grains within the same basin: (i) electrum grains with silver content > 15% and fineness < 850; and (ii) native gold grains with silver content < 10% - 15% and fineness > 850. According to [51] [52] [68] [69], this coexistence in the same sedimentary environment constitutes a strong indication of a dual origin, reflecting the overlap of metamorphic and hydrothermal processes.

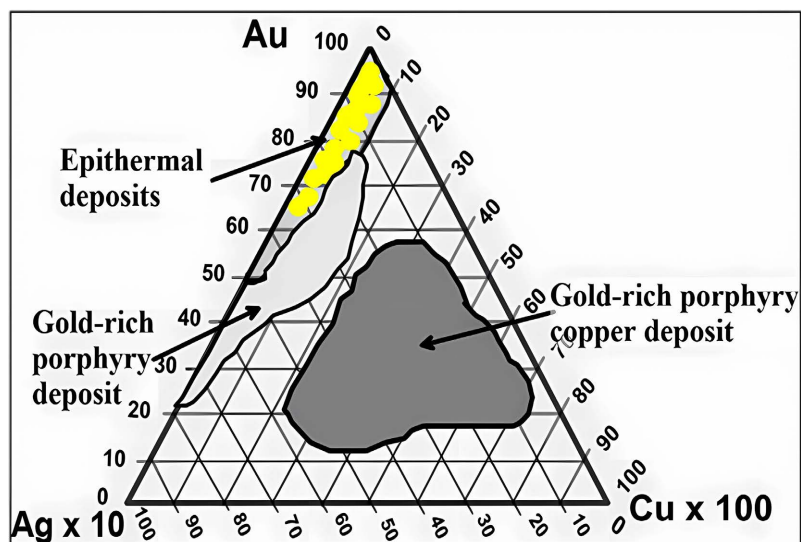


**Figure 11.** Position of the chemistry of the grains analysed in the Au-(Ag × 10)-(Cu × 100) ternary diagram [64] showing a position in the gold-rich epithermal deposits.

- **Composition and Fineness of Gold Grains from the Les Saras Area**

Geochemical analyses highlight two types of gold grains in the Les Saras samples: native gold grains, characterized by high fineness (up to 988) and silver content below 5% (**Table 5**). This type of gold is typical of high-temperature hydrothermal deposits. On the other hand, electrum-type gold grains display lower fineness (down to ~670) and elevated silver content, between 20% and 33% (**Table 5**). These grains generally form in shallower, more oxidizing conditions or in silver-enriched environments (**Figure 12**) [51] [52]. Additionally, the presence of relatively high bismuth concentrations (~0.5% to 1%) also suggests a possible magmatic origin. This chemical signature may indicate an association with bismuth-bearing mineralization linked to magmatic intrusions of the gold-bismuth type. The lack of previous data on gold fineness in the Les Saras area makes these results particularly valuable. Indeed, they provide the first insights into the formation temperatures of gold based on observed fineness values [51]. The data indicate that the presumed gold deposits in the study area formed at high temperatures and considerable depth. The gold present in the ores appears to have high fineness, characteristic of Paleoproterozoic metamorphic rock series belonging to the Loeme, Loukoula, and Bikossi groups. It is also likely that multiple and prolonged metallogenic events contributed to the transformation, purification, and progressive enrichment of the gold. This secondary enrichment possibly results from leaching, particularly observable at the grain boundaries, which removes impurities from the primary gold-bearing minerals. This process increases the gold fineness and alters its geochemical signature. Finally, it is observed that ores poor in sulfides generally display higher fineness compared to those rich in sulfides, confirming the influence of formation conditions [42] [43] [51] [52]. **Figure 12** clearly illustrates the relationship between fineness and temperature in auriferous mineralizations.

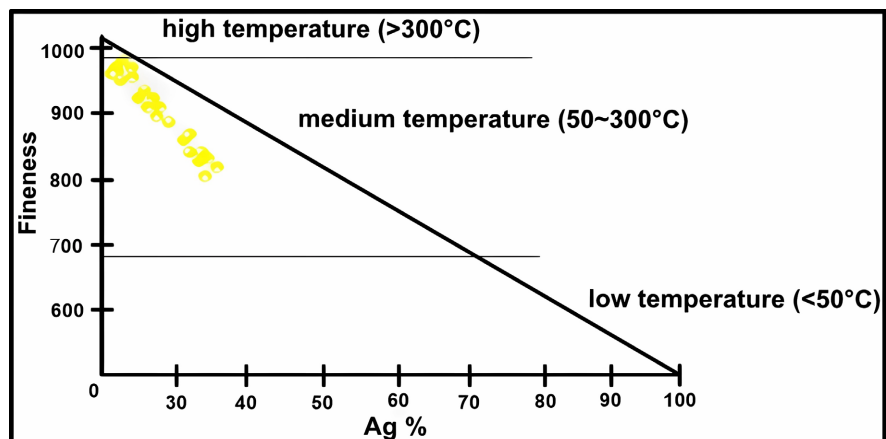


**Figure 12.** Position of Les Saras gold grains in the correlation diagram between gold fineness and mineralization temperature [51] [52].

## 5.2. Geological Processes

Impurities observed in gold grains provide valuable insights into the depositional environment and the nature of the source fluids. The results obtained suggest that

the Les Saras area was influenced by several successive geodynamic events, including regional metamorphism, hydrothermal activity, and various depositional processes. The mineralogical characteristics of ilmenites and garnets confirm the presence of high temperature regional metamorphism, consistent with the regional tectonic framework described by [22] and [32]. Moreover, the enrichment in niobium (Nb), tantalum (Ta), and rare earth elements (REE) detected in the studied grains indicates the involvement of hydrothermal fluids associated with magmatic intrusions. The analysis of gold grain fineness supports the hypothesis of a polymetallic system with a dual origin, involving two distinct types of gold mineralization:

1) Magmatic-hydrothermal origin (high temperature): This type is characterized by very pure native gold (fineness > 950), frequently associated with quartz veins located near felsic intrusions (granitoids, tonalites), formed under hypothermal conditions, at great depth and high temperature (**Figure 12**). This interpretation aligns with the observations reported by [20]-[22]. The presence of bismuth as a trace element in some gold grains suggests a gold-bismuth mineralization type linked to intrusive settings, as discussed by [51] and [52].

2) Volcanogenic or sedimentary origin: This second type is represented by electrum with low fineness (670 - 780), enriched in silver, formed under low-temperature conditions. It is typically associated with sulfide mineralization or secondary alteration processes affecting originally silver-rich rocks. This kind of gold is typical of epithermal transition zones, often located in volcanic settings or reworked sedimentary basins [52]. However, the mineralogy observed shows no sulfides, and there is no evidence of a link with a sedimentary basin. An exhaustive study of the mineralogical record and fluid inclusions is needed to elucidate this problem.

The coexistence of these distinct geochemical signatures within the same area in Les Saras strengthens the hypothesis of a complex metallogenic system involving multiple mineralizing phases, combining deep-sourced inputs with shallow remobilization processes.

### 5.3. Outlook for Mining Explored

The geochemical and morphological characteristics of the Les Saras placers provide valuable clues for mineral exploration. The angular morphology of the gold grains indicates proximity to primary sources. The geochemical signatures of gold, oxides, and silicates suggest a magmatic-hydrothermal and/or volcano-sedimentary origin. These findings can inform exploration efforts within the Loukenene watershed and surrounding areas, supporting the identification of potential targets for exploitation through the application of these signatures in geochemical prospecting.

These results contribute to a better understanding of the mineralogical distribution and geological processes that have influenced the Les Saras placers. Additional analyses will further enhance the interpretation of the origin and mining

potential of these formations.

## 6. Conclusion

This study has enabled the characterization of the gold placers in the Les Saras area, located in the southwest of the Republic of Congo, by identifying their main constituent minerals and tracing their probable geological origin. The results show that the placer mineral assemblage is dominated by oxides (ilmenite, rutile, cassiterite) and includes silicates (garnet), rare earth elements (monazite), and native elements (gold). The morphological characteristics and geochemical signature of the gold grains, along with those of the oxides and silicates, support the hypothesis of an origin linked to epithermal gold-rich deposits. However, the mineral assemblage suggests a mixture of sources: a deep, intrusive, high-temperature source associated with pure native gold enriched in Bi, and a supergene or epithermal source linked to more superficial, silver-rich (electrum) mineralizations. These findings highlight the need for continued exploration of gold-bearing targets in the area. The angular morphology of the gold grains indicates limited transport, suggesting proximity to primary deposits. These observations, combined with the geochemical signatures of oxides and silicates, further support an epithermal origin. These results offer promising prospects for mineral exploration in the Loukenene watershed. The accompanying minerals identified, together with their geochemical signatures, are valuable tools for directing future prospecting campaigns. Further studies should focus on:

- A detailed analysis of fluid inclusions within the placer mineral assemblage.
- Geological and geochemical mapping of adjacent areas to locate primary sources.
- Assessment of the mineralogical and economic potential of the placers at the local scale.

## Acknowledgements

The authors would like to thank the staff of the National Institute of Exact and Natural Sciences (IRSEN) in the Congo and the Laboratoire de GéoRessources in Nancy, France, for carrying out the densimetric separation using dense liquor and the scanning electron microscope (SEM) and microprobe analyses, respectively.

## Conflicts of Interest

The authors declare that there are no conflicts of interest relevant to this study.

## References

- [1] Frimmel, H.E., Tack, L., Basei, M.S., Nutman, A.P. and Boven, A. (2006) Provenance and Chemostratigraphy of the Neoproterozoic West Congolian Group in the Democratic Republic of Congo. *Journal of African Earth Sciences*, **46**, 221-239. <https://doi.org/10.1016/j.jafrearsci.2006.04.010>
- [2] Frimmel, H.E., Basei, M.S. and Gaucher, C. (2010) Neoproterozoic Geodynamic Evo-

- lution of SW-Gondwana: A Southern African Perspective. *International Journal of Earth Sciences*, **100**, 323-354. <https://doi.org/10.1007/s00531-010-0571-9>
- [3] Jébrak, M. (2010) Manual of Géologie. University of Quebec at Montreal, Department of Earth Sciences, Version 3.1, 129.
- [4] Mbenoun, A.M., Ngon, G.F.N., Bayiga, E.C., Fouateu, R.Y. and Bilong, P. (2013) Gold Behavior in Weathering Products of Quartz Vein in Mintom Area South Cameroon (Central Africa). *International Journal of Geosciences*, **4**, 1401-1410. <https://doi.org/10.4236/ijg.2013.410137>
- [5] Mbenoun, A.M., Ngon, G.F.N., Mbog, M.B., Fouateu, R.Y. and Bilong, P. (2021) Study of the Behavior of Gold and Accompanying Chemical Elements in Weathering Profile on a Quartz Vein in Mintom (South Cameroon, Central Africa). *Earth Science Research*, **10**, 54-68. <https://doi.org/10.5539/esr.v10n2p54>
- [6] Mathieu, L. (2015) Indicator Minerals: Garnet, Pyroxene, Spinel, Tourmaline, Olivine and Others. Report, Projet CONSOREM-01, 27.
- [7] Belmedrek, S. (2006) Granulometry and Heavy Minerals of Dune and Beach Sands from the Oued Zhour and Béni Bélaïd Sectors. Ph.D. Thesis, University Mentouri Constantine.
- [8] McClenaghan, M.B. (2011) Overview of Common Processing Methods for Recovery of Indicator Minerals from Sediment and Bedrock in Mineral Exploration. *Geochemistry: Exploration, Environment, Analysis*, **11**, 265-278. <https://doi.org/10.1144/1467-7873/10-im-025>
- [9] Heilbron, M. and Machado, N. (2003) Timing of Terrane Accretion in the Neoproterozoic-Eopaleozoic Ribeira Orogen (se Brazil). *Precambrian Research*, **125**, 87-112. [https://doi.org/10.1016/s0301-9268\(03\)00082-2](https://doi.org/10.1016/s0301-9268(03)00082-2)
- [10] Pedrosa-Soares, A.C., Alkmim, F.F., Tack, L., Noce, C.M., Babinski, M., Silva, L.C., *et al.* (2008) Similarities and Differences between the Brazilian and African Counterparts of the Neoproterozoic Araçuaí-West Congo Orogen. *Geological Society, London, Special Publications*, **294**, 153-172. <https://doi.org/10.1144/sp294.9>
- [11] Pedrosa-Soares, A.C. and de Alkmim, F.F. (2011) How Many Rifting Events Preceded the Development of the Araçuaí-West Congo Orogen? *Geonomos*, **19**, 244-251.
- [12] Fauck, R. (1974) The Factors and Mechanisms of Pedogenesis in Red and Yellow Ferallitic Soils on Sand and Sandstone in Africa, Cah. *ORSTOM*, **XII**, 69-72.
- [13] Jamet, R. (1974) Soil Study with 1/200,000-Scale Map Les Saras. *ORSTOM*, 215.
- [14] Jamet, R. and Rieffel, J.M. (1976) Explanatory Note for the Congo Soil Map 1/200.000. Pointe-Noire sheet and Loubomo sheet *ORSTOM*, 177.
- [15] Schwartz, D. and Lanfranchi, R. (1980) The Origin of Gold Deposits in the Central Mayombe (Congo) Some Hypotheses, Surface Geodynamics, *Pedologist*. *ORSTOM*, 155-160.
- [16] Parisot, J.C., Ventos, V., Grandin, G., Bourges, F., Debat, P., Tollon, F. and Millo, L. (1995) Dynamics of Gold and Other Heavy Minerals in a Cuirass Weathering Profile from Burkina Faso, West Africa, Interest for the Interpretation of the Emplacement of Materials Constituting High Glacis Cuirasses. *Geosciences de Surface*, **321**, 295-302.
- [17] Mpemba-Boni, J. (1990) Contribution to the Study of Ante-Pan Magmatism of the Mayombe Chain. The Example of the Les Saras Massif (SW Congo, Central Africa) Structural Petrology-Geochemistry-Geochronology. Ph.D. Thesis, University of Nancy 1.
- [18] Fullgraf, T., Callec, Y., Thiéblemont, D., Gloaguen, E., Le Métour, J., Boudzoumou,

- F., Delhay-Prat, V., Kebi-Tsoumou, S. and Ndiele, B. (2015) Geological map of the Repub-lic of Congo at 1:200,000, Feuille Dolisie. Editions BRGM, 342.
- [19] Joachim Djama, L.M., Matiaba Bazika, U.V., Boudzoumou, F. and Mouzeo, K. (2018) Petrology and Geodynamic Context of Metabasic Rocks of Nemba Complex in the West Congo Fold Belt (Republic of Congo). *International Journal of Geosciences*, **9**, 1-18. <https://doi.org/10.4236/ijg.2018.91001>
- [20] Bouénitela, V.T.T., Matiaba-Bazika, U.V., Makamba, N.L., Nkodia, H.M.D., Kebi-Tsoumou, S.P.C. and Boudzoumou, F. (2024) An Overview of the Present State of Knowledge in the Tectonostratigraphic Evolution of the West Congo Belt in Republic of Congo. *International Journal of Geosciences*, **15**, 1038-1063. <https://doi.org/10.4236/ijg.2024.1512055>
- [21] Bazika, U.V.M., Bouénitela, V.T.T., Lekeba, N.M. and Boudzoumou, F. (2022) Petrology and Geochemistry of Loukounga Metabasites Rocks: Constraining the Geodynamic Context of Neoproterozoic Nemba Complex in the Mayombe Belt. *Open Journal of Geology*, **12**, 919-946. <https://doi.org/10.4236/ojg.2022.1211044>
- [22] Matiaba-Bazika, U.V., Lekeba Makamba, N., Bouénitela, V.T.T., Tchiguina, N.C.B., Miyouna, T. and Boudzoumou, F. (2024) Geochemical and Petrological Insights into the Neoproterozoic Moumba Metabasites: Implications for Crustal Processes in the West Congo Belt (Republic of Congo). *Journal of Geoscience and Environment Protection*, **12**, 1-29. <https://doi.org/10.4236/gep.2024.122001>
- [23] Tack, L. (2001) Early Neoproterozoic Magmatism (1000-910 Ma) of the Zadinian and Mayumbian Groups (Bas-Congo): Onset of Rodinia Rifting at the Western Edge of the Congo Craton. *Precambrian Research*, **110**, 277-306. [https://doi.org/10.1016/s0301-9268\(01\)00192-9](https://doi.org/10.1016/s0301-9268(01)00192-9)
- [24] Noce, C.M., Pedrosa-Soares, A.C., da Silva, L.C., Armstrong, R. and Piuzana, D. (2007) Evolution of Polycyclic Basement Complexes in the Araçuaí Orogen, Based on U-Pb SHRIMP Data: Implications for Brazil-Africa Links in Paleoproterozoic Time. *Precambrian Research*, **159**, 60-78. <https://doi.org/10.1016/j.precamres.2007.06.001>
- [25] Nsungani, P.C. (2012) The Pan-African Chain of Northwestern Angola: Petro-Structural, Geochemical and Geochronological Study. Implications géodynamiques. Ph.D. Thesis, Université Montpellier II.
- [26] Hossié, G. (1980) Contribution to the Structural Study of Chain. Ph.D. Thesis, University of Montpellier.
- [27] Boudzoumou, F. (1986) The West-Congolian Range and Its Foreland in Congo: Relation to the Mayombian, Sedimentology of Sequences of Upper Proterozoic Age. Ph.D. Thesis, University of Aix Marseille.
- [28] Djama, L.M. (1988) The Mfoubou Granitic Massif and the Guéna Metamorphic Basement (Chaine duMayombe-Congo). Petrology-Geochemistry-Geochronology. Ph.D. Thesis, University of Nancy I.
- [29] Maurin, J.C, Boudzoumou, F., Djama, L.M., Gioan, P., Michard, A., Mpemba-Boni, J., Peucat, J.J., Pin, C. and Vicat, J.P. (1991) The West Congolian Proterozoic Chain and Its Foreland in the Congo: New Geochronological and Structural Data, Implications for Central Africa. *Proceedings of the Academy of Sciences of Paris, II*, **312**, 1327-1334.
- [30] Maurin, J.C. (1993) The West Congolian Pan-African Chain: Correlation with the East Brazilian Domain and Geodynamic Hypothesis. *Journal of Geological Society of France*, **164**, 51-60.
- [31] Dadet, P. (1969) Explanatory Note for the Geological Map of the Republic of Congo Brazzaville at 1:500,000 Scale. BRGM Paris, 107.

- [32] Boudzoumou, F. and Trompette, R. (1988) La chaîne panafricaine ouest-congolienne au Congo (Afrique équatoriale); Un socle polycyclique charrié sur un domaine sub-autochtone formé par l'aulacogène du Mayombe et le bassin de l'Ouest-Congo. *Bulletin de la Société Géologique de France*, **IV**, 889-896. <https://doi.org/10.2113/gssgfbull.iv.6.889>
- [33] Bouénitéla, V.T.T. (2019) The Paleoproterozoic (Eburnian) Domain of the Mayombe Range (Congo-Brazzaville): Origin of and Tectono-Metamorphic Evolution. Ph.D. Thesis, Université de Rennes1, Géosciences.
- [34] Le Bayon, B., Callec, Y., Lasseur, E., Thiéblemont, D., Paquet, F., Gouin, J., Giresse, P., Makolobongo, B., Obambi, U., Mouloundou Niangui, E. and Miassouka Mpika, R. (2015) Geological Map of the Republic of Congo 1:200,000, Conkouati Sheet. Editions BRGM.
- [35] Cosson, J. (1955) Explanatory Note on the Pointe-Noire and Brazzaville Sheets. Geological Map 1:500,000 Scale Reconnaissance Survey. *Journal of the Direction of Mining and Geology of French Equatorial Africa*, 56.
- [36] Vellutini, P., Rocci, G., Vicat, J. and Gioan, P. (1983) Mise en évidence de complexes ophiolitiques dans la chaîne du Mayombe (Gabon—Angola) et nouvelle interprétation géotectonique. *Precambrian Research*, **22**, 1-21. [https://doi.org/10.1016/0301-9268\(83\)90056-6](https://doi.org/10.1016/0301-9268(83)90056-6)
- [37] Affaton, P., Kalsbeek, F., Boudzoumou, F., Trompette, R., Thrane, K. and Frei, R. (2016) The Pan-African West Congo Belt in the Republic of Congo (Congo Brazzaville): Stratigraphy of the Mayombe and West Congo Supergroups Studied by Detrital Zircon Geochronology. *Precambrian Research*, **272**, 185-202. <https://doi.org/10.1016/j.precamres.2015.10.020>
- [38] Daubois, V. (2016) Analysis of Heavy Minerals from Glacial and Fluvio-glacial Sediments in the Clova Region, Ministry of Energy and Natural Resources, Department of Natural Resources. Province of Greville Quebec, 5.
- [39] Watha Ndoudy, N. (1993) Morphological and Geochemical Characteristics of Gold Grains; Application to Prospecting of the Mayoko Placers (Congo). Ph.D. Thesis, INPL Nancy.
- [40] Parfenoff, A., Pomerol, C. and Tourenq, J. (1970) Granular Minerals, Method of Study and Determination. Edition Masson, 578.
- [41] Watha-Ndoudy, N., Okoumel, P.E.W., Miyouna, T., Mpika, R.H.A., Massala, E.G., Mibantsa, G.S., *et al.* (2023) Characterization of Gold Bearing Placers and Associated Minerals in the Elogo Region (North-West Congo Republic). *Open Journal of Geology*, **13**, 287-305. <https://doi.org/10.4236/ojg.2023.135014>
- [42] Boyle, R.W. (1979) The Geochemistry of Gold and Its Deposits. Geological Survey of Canada, 584.
- [43] Metz, P.A. and Hawkins, D.B. (1981) A Summary of Gold Fineness Values from Alaska Placer Deposits. School of Mineral Industry University of Alaska Fairbanks, Alaska 99701. MIRL Report No. 45, 17.
- [44] Essaifi, A., Ballèvre, M., Marniac, C. and Capdevila, R. (2001) Découverte et signification d'une paragenèse à ilménite zincifère dans les métapelites des Jebilet centrales (Maroc). *Comptes Rendus de l'Académie des Sciences—Series IIA—Earth and Planetary Science*, **333**, 381-388. [https://doi.org/10.1016/s1251-8050\(01\)01655-x](https://doi.org/10.1016/s1251-8050(01)01655-x)
- [45] Ercit, T.S., Wise, M.A. and Cerny, P. (1995) Compositional and Structural Systematics of the Columbite Group. *American Mineralogist*, **80**, 613-619. <https://doi.org/10.2138/am-1995-5-619>
- [46] Anderson, M.O., Lentz, D.R., McFarlane, C.R.M. and Falck, H. (2013) A Geological,

- Geochemical and Textural Study of an LCT Pegmatite: Implications for the Magmatic versus Metasomatic Origin of Nb-Ta Mineralization in the Moose II Pegmatite, Northwest Territories, Canada. *Journal of GEOsciences*, **58**, 299-320. <https://doi.org/10.3190/jgeosci.149>
- [47] Ballouard, C., Carr, P., Parisot, F., Gloaguen, É., Melleton, J., Cauzid, J., *et al.* (2024) Petrogenesis and Tectonic-Magmatic Context of Emplacement of Lepidolite and Petalite Pegmatites from the Fregeneda-Almendra Field (Variscan Central Iberian Zone): Clues from Nb-Ta-Sn Oxide U-Pb Geochronology and Mineral Geochemistry. *BSGF—Earth Sciences Bulletin*, **195**, Article 3. <https://doi.org/10.1051/bsgf/2023015>
- [48] Caddick, M.J., Konopásek, J. and Thompson, A.B. (2010) Preservation of Garnet Growth Zoning and the Duration of Prograde Metamorphism. *Journal of Petrology*, **51**, 2327-2347. <https://doi.org/10.1093/petrology/egq059>
- [49] Abreal, A. (2010) Les Grenats des Pegmatites. *Journal of Personal Minearlogist*, **13**, 149-181.
- [50] Abreal, A. (2020) Cristallisation des grenats Influence du manganese. *Journal of Personal Minearlogist*, **14**, 107-125.
- [51] Chao, Y., Yin, J., Yin, Y., Shi, H. and Xiang, S. (2022) Occurrence State and Properties of Gold Minerals from the Gold Deposits on the North China Platform. *European Journal of Applied Sciences*, **10**, 504-513.
- [52] Nikiforova, Z. (2024) Mineralogical Method as an Effective Way to Predict Gold Ore Types of Deposits in Platform Areas (East of the Siberian Platform). *Minerals*, **14**, Article 631. <https://doi.org/10.3390/min14060631>
- [53] Chapman, R.J., Leake, R.C., Warner, R.A., Cahill, M.C., Moles, N.R., Shell, C.A., *et al.* (2006) Microchemical Characterisation of Natural Gold and Artefact Gold as a Tool for Provenancing Prehistoric Gold Artefacts: A Case Study in Ireland. *Applied Geochemistry*, **21**, 904-918. <https://doi.org/10.1016/j.apgeochem.2006.01.007>
- [54] Shuster, J., Lengke, M., Márquez-Zavalía, M.F. and Southam, G. (2016) Floating Gold Grains and Nanophase Particles Produced from the Biogeochemical Weathering of a Gold-Bearing Ore. *Economic Geology*, **111**, 1485-1494. <https://doi.org/10.2113/econgeo.111.6.1485>
- [55] Townley, B.K., Hérail, G., Maksaev, V., Palacios, C., Parseval, P.d., Sepulveda, F., *et al.* (2003) Gold Grain Morphology and Composition as an Exploration Tool: Application to Gold Exploration in Covered Areas. *Geochemistry: Exploration, Environment, Analysis*, **3**, 29-38. <https://doi.org/10.1144/1467-787302-042>
- [56] Masson, F., Beaudoin, G. and Laurendeau, D. (2020) Quantification of the Morphology of Gold Grains in 3D Using X-Ray Microscopy and SEM Photogrammetry. *Journal of Sedimentary Research*, **90**, 286-296. <https://doi.org/10.2110/jsr.2020.16>
- [57] Lalomov, A., Grigorieva, A., Kotov, A. and Ivanova, L. (2023) Typomorphic Features and Source of Native Gold from the Sykhoi Log Area Placer Deposits, Bodaibo Gold-Bearing District, Siberia, Russia. *Minerals*, **13**, Article 707. <https://doi.org/10.3390/min13050707>
- [58] de Oliveira, S.M.B. and de Oliveira, N.M. (2000) The Morphology of Gold Grains Associated with Oxidation of Sulphide-Bearing Quartz Veins at São Bartolomeu, Central Brazil. *Journal of South American Earth Sciences*, **13**, 217-224. [https://doi.org/10.1016/s0895-9811\(00\)00021-3](https://doi.org/10.1016/s0895-9811(00)00021-3)
- [59] Hérail, G., Fornari, M., Viscarre, G. and Mirande, V. (1990) Morphologique et évolution chimique des grains d'or lors de la formation d'un placer fluviatile polygénique: L'exemple du placer Mio-Pléistocène Tipuani (Bolivie). *Chronique de la Recherche*

*Minière*, **500**, 41-49.

- [60] Auger, C.C. (2016) Chemical Composition of Indicator Minerals from the Kittilä Mine. Master's Thesis, Laval University.
- [61] Bruni, Y. and Hatert, F. (2017) Étude minéralogique de l'or et de ses minéraux accompagnateurs sur le pourtour du massif cambro-ordovicien de Serpont, Belgique. *Bulletin de la Société Royale des Sciences de Liège*, **86**, 113-168. <https://doi.org/10.25518/0037-9565.7243>
- [62] Dilabio, R.N.W. (1991) Classification and Interpretation of the Shapes and Surface Textures of Gold Grains from Till. In: Herail, G. and Fornari, M., Eds., *Gisements alluviaux d'or*, ORSTOM, 297-313.
- [63] Groen, J.C., Craig, J.R. and Rimstidt, J.D. (1990) Gold-Rich Rim Formation on Electrum Grains in Placers. *Canadian Mineralogist*, **28**, 207-228.
- [64] Fairbrother, L., Brugger, J., Shapter, J., Laird, J.S., Southam, G. and Reith, F. (2012) Supergene Gold Transformation: Biogenic Secondary and Nano-Particulate Gold from Arid Australia. *Chemical Geology*, **320**, 17-31. <https://doi.org/10.1016/j.chemgeo.2012.05.025>
- [65] Palacios, C., Herail, G., Townley, B., Maksaev, V., Sepulveda, F., de Parseval, P., *et al.* (2001) The Composition of Gold in the Cerro Casale Gold-Rich Porphyry Deposit, Maricunga Belt, Northern Chile. *The Canadian Mineralogist*, **39**, 907-915. <https://doi.org/10.2113/gscanmin.39.3.907>
- [66] Phelps, P.R., Lee, C.A. and Morton, D.M. (2020) Episodes of Fast Crystal Growth in Pegmatites. *Nature Communications*, **11**, Article No. 4986. <https://doi.org/10.1038/s41467-020-18806-w>
- [67] Anand, R., Lintern, M., Hough, R., Noble, R., Verrall, M., Salama, W., *et al.* (2017) The Dynamics of Gold in Regolith Change with Differing Environmental Conditions over Time. *Geology*, **45**, 127-130. <https://doi.org/10.1130/g38591.1>
- [68] Yesares, L., Aiglsperger, T., Sáez, R., Almodóvar, G.R., Nieto, J.M., Proenza, J.A., *et al.* (2015) Gold Behavior in Supergene Profiles under Changing Redox Conditions: The Example of the Las Cruces Deposit, Iberian Pyrite Belt. *Economic Geology*, **110**, 2109-2126. <https://doi.org/10.2113/econgeo.110.8.2109>
- [69] Groves, D.I., Santosh, M., Müller, D., Zhang, L., Deng, J., Yang, L., *et al.* (2022) Mineral Systems: Their Advantages in Terms of Developing Holistic Genetic Models and for Target Generation in Global Mineral Exploration. *Geosystems and Geoenvironment*, **1**, Article ID: 100001. <https://doi.org/10.1016/j.geogeo.2021.09.001>